LETTERS

Eruptions arising from tidally controlled periodic openings of rifts on Enceladus

T. A. Hurford[1], P. Helfenstein[2], G. V. Hoppa[3], R. Greenberg[4] & B. G. Bills[1,5]

In 2005, plumes were detected near the south polar region of Enceladus[1], a small icy satellite of Saturn. Observations of the south pole revealed large rifts in the crust, informally called 'tiger stripes', which exhibit higher temperatures than the surrounding terrain and are probably sources of the observed eruptions[2]. Models of the ultimate interior source for the eruptions are under consideration[1,3–5]. Other models of an expanding plume[6] require eruptions from discrete sources, as well as less voluminous eruptions from a more extended source, to match the observations. No physical mechanism that matches the observations has been identified to control these eruptions. Here we report a mechanism in which temporal variations in tidal stress open and close the tiger-stripe rifts, governing the timing of eruptions. During each orbit, every portion of each tiger stripe rift spends about half the time in tension, which allows the rift to open, exposing volatiles, and allowing eruptions. In a complementary process, periodic shear stress along the rifts also generates heat along their lengths[7–9], which has the capacity to enhance eruptions. Plume activity is expected to vary periodically, affecting the injection of material into Saturn's E ring[10] and its formation, evolution and structure. Moreover, the stresses controlling eruptions imply that Enceladus' icy shell behaves as a thin elastic layer, perhaps only a few tens of kilometres thick.

Enceladus is a small (radius ~250 km) moon that orbits Saturn between the moons Mimas and Tethys with a period of 1.37 days. This proximity to Saturn means that tidal dissipation should have quickly circularized the orbit. However, a 2:1 mean motion resonance with the moon Dione, which orbits just beyond Tethys, excites the orbital eccentricity to the observed value of 0.0047, which in turn produces periodic tidal stress on the surface.

A thin-shell approximation yields the surface stresses from the tidal deformation of a thin, elastic outer layer[11], assuming that this layer is decoupled from the deeper interior of the body (for example, by a fluid layer[12,13]). Thus there is negligible shear between the elastic shell and the interior. The thin-shell approximation of surface stress is valid as long as the elastic outer layer is not thick enough to begin significantly hampering tidal deformation of the body. For Europa, the stresses in an icy elastic outer layer of $<$15 km have been shown not to differ significantly from the thin-shell approximation of surface stress[14]. The thin elastic layer deforms to fit the tidal figure of the body's interior. The horizontal strain of this shell, as required to fit the tidally distorted interior, produces stress on the surface, given by:

$$\sigma_{\theta\theta} = (3M\mu h_2/8\pi\rho_{av}a^3)(1+\nu)/(5+\nu)(5+3\cos 2\theta) \quad (1)$$

and

$$\sigma_{\varphi\varphi} = -(3M\mu h_2/8\pi\rho_{av}a^3)(1+\nu)/(5+\nu)(1-9\cos 2\theta) \quad (2)$$

where θ is the angular distance measured with respect to the tidal distortion's axis of symmetry (ostensibly the sub-anti-saturnian line)[15,16]. The quantity $\sigma_{\theta\theta}$ is the stress along the surface in the direction radial to the tidal bulges, while $\sigma_{\varphi\varphi}$ is the stress along the surface in a direction orthogonal to the $\sigma_{\theta\theta}$ stress. In these expressions μ is the rigidity of the shell, ν is Poisson's ratio, ρ_{av} is the average density of the body, and M is the mass of Saturn, the tide-raiser, which is a distance a from the centre of the deformed body. The magnitude of the tidal stress on the surface is proportional to the Love number h_2, which is a constant of proportionality that governs the tidal deformation of the body, and is determined by its internal structure.

Enceladus' finite eccentricity causes small daily changes in a and θ. For example, during Enceladus' orbit, between pericentre and apocentre, the change in distance from Saturn produces a small variation in the height of the main tide with an amplitude of $(9eh_2MR)/(4\rho_{av}a^3)$, where R is Enceladus' radius and e is its eccentricity. In addition to the change in the amplitude of the tide, Saturn's angular position with respect to a fixed location above Enceladus' surface oscillates with an amplitude of $2e$ radians east and west, changing

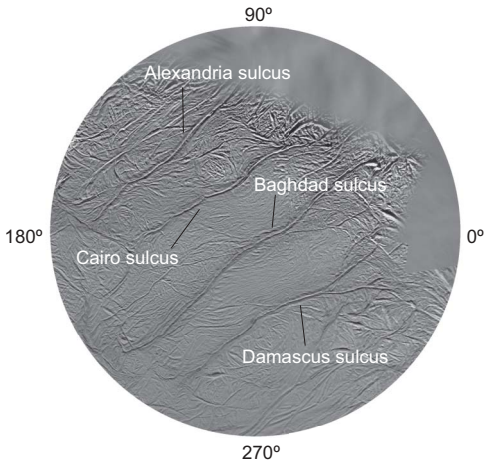

Figure 1 | The south polar region of Enceladus. This image from a high-resolution atlas[21] of Enceladus shows the south polar region from 65° S poleward. These features are typically about 130 km in length, 2 km wide, with a trough 500 m deep, and are flanked on each side by ridges 100 m tall[1]. One of these features (Cairo sulcus) has arcuate segments similar to the cycloidal ridges on Europa[22], where distinctive cycloidal patterns were probably produced by periodic tidal stresses[14,23]. The similar shape suggests a similar formation process controlled by diurnal tidal stresses[22].

[1]Planetary Geodynamics Laboratory, NASA Goddard Space Flight Center, Greenbelt, Maryland 20771, USA. [2]CRSR, Cornell University, Ithaca, New York 14853, USA. [3]Raytheon, Woburn, Massachusetts 01801, USA. [4]Lunar and Planetary Laboratory, University of Arizona, Tucson, Arizona 85721, USA. [5]Institute for Geophysics and Planetary Physics, Scripps Institution of Oceanography, La Jolla, California 92093, USA.

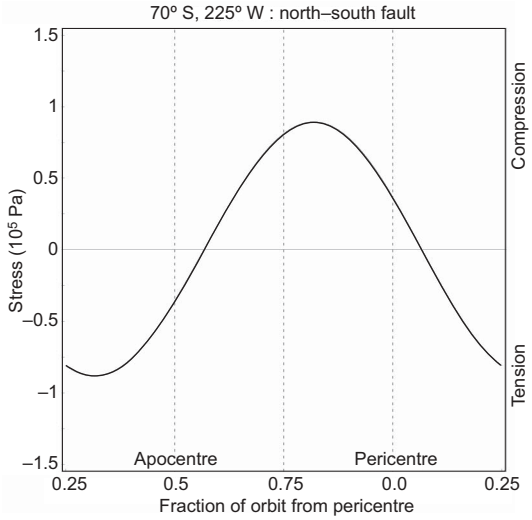

Figure 2 | Stress normal to a north–south-oriented fault. The stress across this fault, which is oriented north–south at a latitude of 70° S and longitude of 225° W is shown. At pericentre the fault is being held closed, because the stress normal to it is compressive. However, as Enceladus orbits, the stress changes from compression to tension, allowing the fault to open, possibly exposing liquid water or other volatiles and creating an eruption. The fault remains in tension for half of an orbit, at which point the normal stress once again becomes compressive, forcing the crack to close, ending any possibility of an eruption.

the angular distance to the tidal bulge θ slightly. These two effects combine, yielding the diurnally varying part of the tide.

For a water-ice crust, we used the plausible values of the elastic parameters[17] $\mu = 3.52 \times 10^9$ Pa and $\nu = 0.33$, and assumed a conservative value for the tidal response given by $h_2 = 0.32$, which corresponds to a diurnal tidal amplitude of ~5 m when $3M/8\rho_{av}a^3 = 0.01$.

In a method similar to that used to consider stress along cracks on the moon Europa's surface[18], diurnal variation in the surface stress normal to a fault can be calculated (Fig. 2). Tension across a fault opens the feature, allowing pent-up volatiles to be released and eruptions to occur. The time of this release depends on the orientation of the fault and its location. Similar analysis of the stresses normal to the fault can be made all along each tiger-stripe feature near the south pole and comparisons with plume observations can be done to see if any of the features are in tension during the observational sequences.

It was hypothesized that similar venting might be observed on Europa, so the Galileo spacecraft imaging team included a sequence specifically designed to search for plumes. However, at the time and place of those observations, the area imaged was under tidal compression—the least likely condition for venting—and no plumes were detected[19]. In view of this, we can address whether the stress state of the cracks on Enceladus was conducive to venting at the times of the Cassini imaging.

The plume activity on Enceladus was observed at different locations in its orbit during imaging sequences that lasted about an hour. During the January observation, Enceladus was about an eighth of an

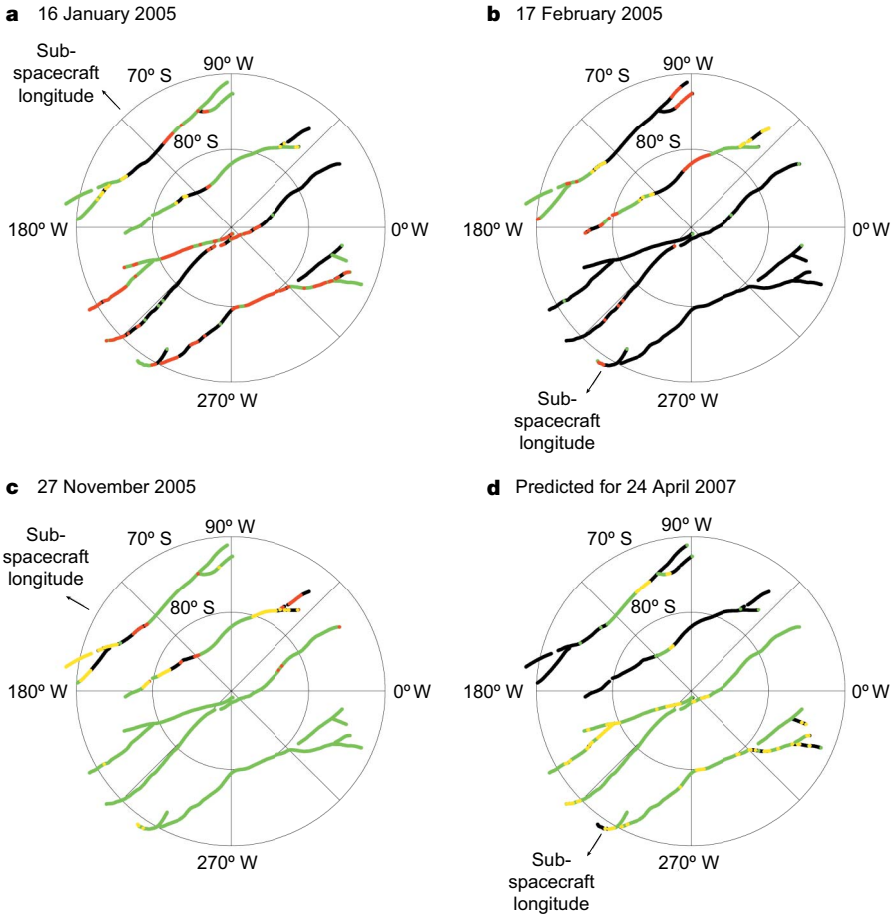

Figure 3 | The stress state across the tiger stripe rifts. During observation sequences from 2005 the stress along each rift is shown (**a**–**c**), along with the predicted state during the proposed April 2007 observation (**d**). The colour indicates the stress state. Black means that some portion of the feature was in compression during the entire imaging sequence, while green means that it was in tension. Yellow indicates that the stress switched from compression to tension, opening the rift during the imaging sequence, and orange indicates that the stress switched from tension to compression, potentially closing the rift.

orbit past apocentre and 46% of the tiger stripes were in tension for the hour-long imaging sequence (Fig. 3a). Tiger stripes between 225° W and 45° W longitude (11% of the rift system) experienced a switch to compression. This observation was scheduled during the part of the orbit when the rifts were in the process of closing as the stresses became compressive. Hence, during the February (Fig. 3b) observations, taken at about at an eighth of an orbit before pericentre, only 16% of the tiger stripes remained in tension while more of the system (4%) switched to compression. We would therefore expect the plume activity in the February detection to be less intense than in the plumes of January, but the different viewing geometries make direct comparisons between the observations difficult, because particles in the plumes are strongly forward-scattering and the intensity of scattered light from the plumes dramatically increases with increasing phase angle. Finally, during the November observation sequence, taken near apocentre (Fig. 3c), 82% of the tiger stripes experienced tension during the imaging sequence.

The three observations of plumes near the south pole show a progression as Enceladus orbits from apocentre towards pericentre. In November, with Enceladus near apocentre, almost the entire region is experiencing tension along the rifts (Fig. 3c). In January, the rifts are beginning to close after passing apocentre, beginning with Damascus sulcus and Baghdad sulcus (Fig. 3a). As Enceladus approaches pericentre, most of the system is in compression (Fig. 3b). We predict that activity should be lowest when Enceladus is near pericentre and highest when Enceladus is near apocentre (see the Supplementary Information).

Because most of the system is in tension during the November observations, jets can be observed erupting nearly anywhere along the rifts (see Supplementary Information). However, if tides control the eruption process, we predict that improved triangulation methods[20] will find that the observed jets are not distributed evenly throughout the rift system. The location of jets may be controlled by tides in two different ways. First, if jets occur where a rift first opens in tension, allowing the pent-up volatiles to erupt, favoured recent jet locations will be found along Alexandria sulcus near 160° W, 72° S, along Cairo sulcus near 170° W, 77° S and 50° W, 75° S, along Baghdad sulcus near 210° W, 70° S and along Damascus sulcus near 240° W, 70° S. Second, tidal stress levels may influence the locations where jetting occurs. The locations along each rift where tidal stresses are close to their maxima are near 105° W, 74° S along Alexandria sulcus, near 115° W, 84° S along Cairo sulcus, near 315° W, 89° S along Baghdad sulcus and near 275° W, 80° S along Damascus sulcus. Thus, of these locations, the ones in Baghdad sulcus and Damascus sulcus opened earlier than the locations along the other two rifts and Baghdad sulcus or Damascus sulcus or both are the most likely sources for the November jets.

A Cassini imaging sequence now planned for 24 April 2007 would take place over about 1.5 h, while Enceladus is about one-fifth of an orbit past pericentre (Fig. 3d). We find that during this time 57% of the tiger stripes will be in tension. Like the November plume observation, a significant portion (6%) of the features will be in the process of opening up as the tension across them changes from compression to tension.

On the basis of the geometry of the imaging sequence in April, sources for plumes erupting from the region of Baghdad sulcus, Alexandria sulcus and Cairo sulcus will be difficult to locate on the surface. Without the surface being resolved in the image a plume in that region could originate from Baghdad sulcus in the foreground or Alexandria sulcus in the background. However, activity from Damascus sulcus should be observationally distinct from the rest of the tiger-stripe rift system and the rift will have recently experienced tension, providing an opportunity to observe the beginning stages of eruptions on Enceladus and test the two scenarios described above. If eruptions are controlled by the release of pent-up volatiles, this observational sequence could reveal an especially active phase as pent-up volatiles begin to erupt along Damascus. However, if stresses near their maxima control the formation of jets then this rift may be observed to be inactive.

Received 29 November 2006; accepted 30 March 2007.

1. Porco, C. C. *et al.* Cassini observes the active south pole of Enceladus. *Science* **311,** 1393–1401 (2006).
2. Spencer, J. R. *et al.* Cassini encounters Enceladus: background and the discovery of a south polar hot spot. *Science* **311,** 1401–1405 (2006).
3. Nimmo, F. & Pappalardo, R. T. Diapir-induced reorientation of Saturn's moon Enceladus. *Nature* **441,** 614–616 (2006).
4. Collins, G. & Goodman, J. C. Internal melting and the shape of Enceladus. *AAS/Division Planet. Sci. Conf.* **38,** abstr. 18.03 (American Astronomical Society, 2006).
5. Kieffer, S. *et al.* A clathrate reservoir hypothesis for Enceladus' south polar plume. *Science* **314,** 1764–1766 (2006).
6. Ingersoll, A. P., Porco, C. C., Helfenstein, P., West, R. A. & the Cassini ISS Team. Models of the Enceladus plumes. *AAS/Division Planet. Sci. Conf.* **38,** abstr. 15.02 (American Astronomical Society, 2006).
7. Nimmo, F. & Gaidos, E. Strike-slip motion and double ridge formation on Europa. *J. Geophys. Res.* **107,** doi:10.1029/2000JE001476 (2002).
8. Prockter, L. M., Nimmo, F. & Pappalardo, R. T. A shear heating origin for ridges on Triton. *Geophys. Res. Lett.* **32,** doi:10.1029/2005GL022832 (2005).
9. Nimmo, F., Spencer, J. R., Pappalardo, R. T. & Mullen, M. E. Shear heating as the origin of the plumes and heat flux on Enceladus. *Nature* doi:10.1038/nature05783 (this issue).
10. Horanyi, M., Burns, J. A. & Hamilton, D. P. The dynamics of Saturn's E ring particles. *Icarus* **97,** 248–259 (1992).
11. Giese, B., Roatsch, T., Wagner, R., Denk, T. & Neukum, G. Topographic models of the icy Saturn satellites. *Eur. Planet. Sci. Congr.* abstr. 119 (2006).
12. Sohl, F., Hussmann, H. & Ziethe, R. Interior structures of Enceladus and Mimas: implications from their densities and equilibrium shapes. *AAS/Division Planet. Sci. Conf.* **38,** abstr. 24.01 (American Astronomical Society, 2006).
13. Hussmann, H., Sohl, F. & Grott, M. Tidal heating in Enceladus And Mimas: implications for their thermal and orbital states. *AAS/Division Planet. Sci. Conf.* **38,** abstr. 24.02 (American Astronomical Society, 2006).
14. Hurford, T. A. *Tides and Tidal Stress: Applications to Europa*. PhD thesis, Univ. Arizona (2005).
15. Melosh, H. J. Global tectonics of a despun planet. *Icarus* **31,** 221–243 (1977).
16. Leith, A. C. & McKinnon, W. B. Is there evidence for polar wander on Europa? *Icarus* **120,** 387–398 (1996).
17. Gammon, P. H., Kiefte, H., Clouter, M. J. & Denner, W. W. Elastic constants of artificial and natural ice samples by Brillouin spectroscopy. *J. Glaciol.* **29,** 433–460 (1983).
18. Hoppa, G., Tufts, B. R., Greenberg, R. & Geissler, P. Strike-slip faults on Europa: global shear patterns driven by tidal stress. *Icarus* **141,** 287–298 (1999).
19. Hoppa, G. V., Greenberg, R., Tufts, B. R. & Geissler, P. E. Plume detection on Europa: locations of favorable tidal stress. *Lunar Planet. Inst. Conf.* **30,** abstr. 1603 (1999).
20. Porco, C. *et al.* Enceladus' jets: particle characteristics, surface source locations, temporal variability, and correlations with thermal hot spots. *Lunar Planet. Inst. Conf.* **38,** abstr. 2310 (2007).
21. Roatsch, T. *et al.* High resolution Enceladus atlas derived from Cassini-ISS images. *Planet. Space Sci.* (submitted).
22. Hurford, T. A., Greenberg, R. & Hoppa, G. V. South polar cycloidal rift on Enceladus. *AAS/Division Planet. Sci. Conf.* **38,** abstr. 18.04 (American Astronomical Society, 2006).
23. Hoppa, G. V., Tufts, B. R., Greenberg, R. & Geissler, P. E. Formation of cycloidal features on Europa. *Science* **285,** 1899–1902 (1999).

Supplementary Information is linked to the online version of the paper at www.nature.com/nature.

Acknowledgements This work was supported by the NASA Posdoctoral Program (NPP) under the administration of Oak Ridge Associated Universities (ORAU).

Author Information Reprints and permissions information is available at www.nature.com/reprints. The authors declare no competing financial interests. Correspondence and requests for materials should be addressed to T.A.H. (hurfordt@core2.gsfc.nasa.gov).